NASA/TM-20240002413

Space Exposure of Indium Tin Oxide Coatings

Henry C. de Groh III, Kim K. de Groh, and Skyler J. Gregor
Glenn Research Center, Cleveland, Ohio

Bruce A. Banks
Science Applications International Corporation, Cleveland, Ohio

March 2024

NASA STI Program Report Series

Since its founding, NASA has been dedicated to the advancement of aeronautics and space science. The NASA scientific and technical information (STI) program plays a key part in helping NASA maintain this important role.

The NASA STI program operates under the auspices of the Agency Chief Information Officer. It collects, organizes, provides for archiving, and disseminates NASA's STI. The NASA STI program provides access to the NTRS Registered and its public interface, the NASA Technical Reports Server, thus providing one of the largest collections of aeronautical and space science STI in the world. Results are published in both non-NASA channels and by NASA in the NASA STI Report Series, which includes the following report types:

- TECHNICAL PUBLICATION.
  Reports of completed research or a major significant phase of research that present the results of NASA Programs and include extensive data or theoretical analysis. Includes compilations of significant scientific and technical data and information deemed to be of continuing reference value. NASA counterpart of peer-reviewed formal professional papers but has less stringent limitations on manuscript length and extent of graphic presentations.

- TECHNICAL MEMORANDUM.
  Scientific and technical findings that are preliminary or of specialized interest, e.g., quick release reports, working papers, and bibliographies that contain minimal annotation. Does not contain extensive analysis.

- CONTRACTOR REPORT.
  Scientific and technical findings by NASA-sponsored contractors and grantees.

- CONTRACTOR REPORT.
  Scientific and technical findings by NASA-sponsored contractors and grantees.

- CONFERENCE PUBLICATION.
  Collected papers from scientific and technical conferences, symposia, seminars, or other meetings sponsored or co-sponsored by NASA.

- SPECIAL PUBLICATION.
  Scientific, technical, or historical information from NASA programs, projects, and missions, often concerned with subjects having substantial public interest.

- TECHNICAL TRANSLATION.
  English-language translations of foreign scientific and technical material pertinent to NASA's mission.

Specialized services also include organizing and publishing research results, distributing specialized research announcements and feeds, providing information desk and personal search support, and enabling data exchange services.

For more information about the NASA STI program, see the following:

- Access the NASA STI program home page at http://www.sti.nasa.gov

NASA/TM-20240002413

Space Exposure of Indium Tin Oxide Coatings

Henry C. de Groh III, Kim K. de Groh, and Skyler J. Gregor
Glenn Research Center, Cleveland, Ohio

Bruce A. Banks
Science Applications International Corporation, Cleveland, Ohio

National Aeronautics and
Space Administration

Glenn Research Center
Cleveland, Ohio 44135

March 2024

Acknowledgments

We are grateful to the NASA Flight Opportunities program, the International Space Station Program Office and Aegis Aerospace for making this flight opportunity possible. We would also like to thank Diane Malarik of NASA Headquarters, along with Craig Robinson and Kelly Bailey of NASA Glenn Research Center for their long-term support of this MISSE-FF experiment. We would also like to thank Nathan Baier of Sheldahl for providing the ITO film. This work is supported by the NASA Biological and Physical Sciences Division.

Level of Review: This material has been technically reviewed by technical management.

This report is available in electronic form at https://www.sti.nasa.gov/ and https://ntrs.nasa.gov/

NASA STI Program/Mail Stop 050
NASA Langley Research Center
Hampton, VA 23681-2199

Space Exposure of Indium Tin Oxide Coatings

Henry C. de Groh III*, Kim K. de Groh, and Skyler J. Gregor†
National Aeronautics and Space Administration
Glenn Research Center
Cleveland, Ohio 44135

Bruce A. Banks‡
Science Applications International Corporation
Cleveland, Ohio 44135

Abstract

Indium tin oxide (ITO) coated thermal control samples were exposed to the space environment as part of the Materials International Space Station Experiment-9 (MISSE-9) mission to assess the impact of low Earth orbit (LEO) on material properties. Six samples were flown as part of the Polymers and Composites Experiment-1 (PCE-1): four samples of ITO coated silver Teflon (FEP/Ag/Inconel), and two samples of ITO coated Kapton® HN (Kapton HN/Al). Samples were flown in ram, wake and zenith directions and were directly exposed to space for 0.77 years (ram) or 0.54 years (wake and zenith). Flight and corresponding control samples were tested post flight for changes in optical properties (total reflectance and solar absorptance) and film electrical resistance. In addition, the atomic oxygen erosion yield (E_y) was determined for each flight sample. This paper provides details on the flight sample materials, the mission space exposure and the post-flight test results. Indium tin oxide coated samples were not significantly damaged by the LEO exposures. The atomic oxygen E_y values were very low and the solar absorptance changed very little. Sheet resistance of the ITO coated Kapton HN/Al doubled after ram exposure, however its final resistance of 10,820 Ohm/square is believed to be low enough to enable dissipation of electrostatic charges. Sheet resistance measurements for the ITO coated FEP/Ag/Inconel sheets suffered from high levels of scatter, with some resistance measurements higher than 370,000 Ohms/square.

1.0 Introduction

While in orbit, spacecraft are exposed to charged particle fluxes that can lead to high electrostatic charges and arcing, resulting in damage to the spacecraft. Indium tin oxide (ITO) is a conductive transparent oxide used in spacecraft thermal control sheet material to dissipate these electrostatic charges [1,2]. A thin film of ITO is typically deposited on a multilayer flexible sheet substrate such as Teflon® fluorinated ethylene propylene (FEP) or Kapton® with a reflective back layer made of aluminum or silver. These sheets are used on the outside of spacecraft to help maintain optimal operating temperatures. However, while in low Earth orbit (LEO), exposed

*Currently retired
†Summer 2022 Pathways Intern at NASA Glenn Research Center
‡Currently retired

materials are subjected to a variety of environmental hazards such as atomic oxygen (AO) and ultraviolet (UV) radiation; these can cause damage and changes in material properties [3,4]. To assess the impact of LEO on the properties of ITO thermal control materials, a variety of ITO coated sheet materials were exposed to LEO as part of the Polymers and Composites Experiment-1 (PCE-1) [3]. The PCE-1 was flown as part of the Materials International Space Station Experiment-9 (MISSE-9) mission, which was launched April 2, 2018 on SpaceX-14 and returned January 7, 2020 on SpaceX-19 [3]. The flight samples were flown in MISSE Sample Carriers (MSCs) attached to the MISSE-Flight Facility (MISSE-FF) through use of the International Space Station's (ISS) robot arm.

2.0 Materials

Indium tin oxide coatings, approximately 10 nm thick, were placed on top of two different multilayer substrate film materials:

- *Kapton® HN (0.002 in. (0.051 mm) thick) with vapor deposited aluminum (VDA) on the backside.*
- *Teflon® fluorinated ethylene propylene (FEP, 0.005 in. (0.127 mm) thick) with silver then Inconel on the backside. This material is known as Silver-Teflon.*

These ITO materials were supplied as sheets from Multek Flexible Circuits (Northfield MN, www.sheldahl.com) and cut into 1.0 in. (2.54 cm) square flight and control (backup) samples. The PCE-1 ITO flight samples along with the mission flight orientation, MISSE-9 sample identification, material, material abbreviation and film thickness are provided in Table 1. The 1 in. (25.4 mm) square sheet flight samples (F) were placed in the MSC deck "picture frame holders" with 0.827 in. (21 mm) square openings as shown in Figure 1. Identical backup samples of each were cut from the same sheet materials and served as backup (B) or control samples in post-flight testing.

Table 1. MISSE-9 PCE-1 Indium Tin Oxide (ITO) Flight Samples

Flight Orientation	MISSE-9 ID	Material	Abbreviation	Polymer Thickness (inch)
Ram	M9R-S5 F	ITO coated Kapton HN/aluminum	ITO/Kapton HN/Al	0.002
	M9R-S6 F	ITO coated Silver-Teflon	ITO/FEP/Ag/Inconel	0.005
Wake	M9W-S1 F	ITO coated Kapton HN/aluminum	ITO/Kapton HN/Al	0.002
	M9W-S2 F	ITO coated Silver-Teflon	ITO/FEP/Ag/Inconel	0.005
	M9W-S3 F	ITO coated Silver-Teflon	ITO/FEP/Ag/Inconel	0.005
Zenith	M9Z-S5 F	ITO coated Silver-Teflon	ITO/FEP/Ag/Inconel	0.005

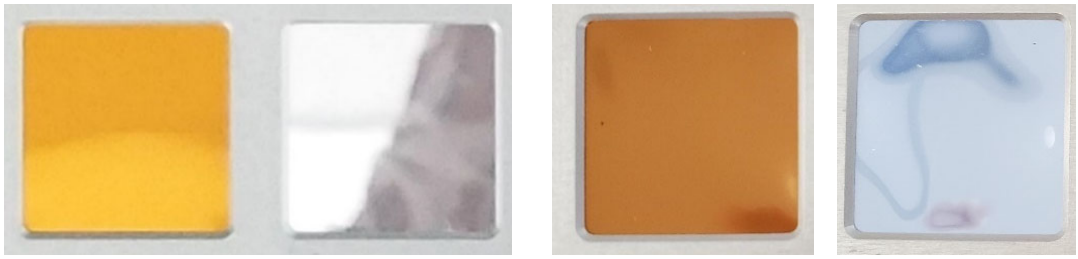

Pre-Flight Post-Flight

a.

Pre-Flight

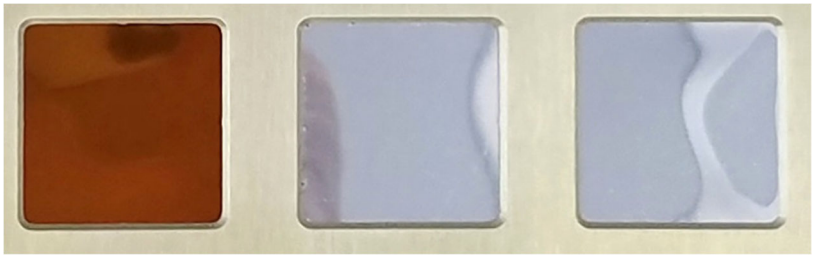

Post-Flight

b.

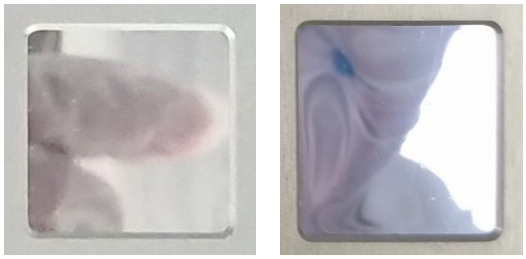

Pre-Flight Post-Flight

c.

Figure 1. Pre-flight and post-Flight images of the MISSE-9 flight samples in their 21 mm square picture frame style holders: (a) Ram ITO samples M9R-S5 (bronze) and M9R-S6 (silvery): Pre-flight on left and post-flight on right, (b) Wake ITO samples M9W-S1 (left), M9W-S2 (center) and M9W-S3 (right): Pre-flight on the top and post-flight on the bottom, and (c) Zenith ITO sample M9Z-S5: Pre-Flight on left and post-flight on right.

3.0 Experimental Procedures

3.1 Film Resistance Measurements

The Ohms/square sheet resistance of the ITO coated films was measured using an Ossila Four-Point Probe from CMC Microsystems, which is shown in Figure 2. To measure the sheet resistance, a sample was placed under the probes near the center. Once the probes were lowered onto the sample, a measurement would be made and analyzed using the accompanying software. To make another measurement, the probes were then lowered further, hence increasing the pressure on the film sample. The probes were then lowered further, increasing their pressure on the film sample, and the measurement repeated. Probe pressure was increased until a valid resistance measurement was achieved. Sheet resistance values were found to vary extensively among the different samples as well as within a given sample. The number of times the resistance of a sample was measured was at least three, but if results were not consistent many more measurements were taken over a variety of areas and averaged. The equipment used, as far as we know, was not calibrated after being set up at NASA Glenn; nor was a standard available to test the accuracy of the equipment. Thus, absolute accuracy of the resistance measurements is unknown, however we believe the relative resistance results show meaningful trends.

3.2 Optical Properties

A Cary 5000 Spectrophotometer with a DRA-2500 integrating sphere attachment was used to collect optical data for the post-flight samples and their controls. The spectrophotometer was back corrected with a Spectralon 99% reflectance standard from Labsphere. Total reflectivity (TR_λ) was measured for all samples over the range of wavelengths 250 to 2500 nm. A NASA Glenn Research Center Cary 5000 Excel® Macro was used to compute the spectral absorptance (α_λ), which was determined using the equation $\alpha_\lambda = 1 - TR_\lambda$. The Excel® Macro was also used to integrate each spectral curve into the air mass zero (AM0) solar spectrum over the spectral range (250 to 2500 nm) to get the total AM0 integrated total reflectance (TR) and solar absorptance (α_s) for each flight and control sample [5,6].

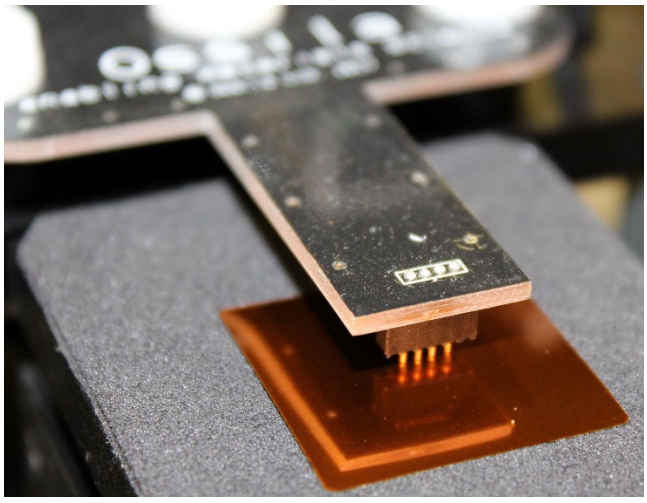

Figure 2. ITO sample with the Ossila Four-Point Probe used to measure sheet resistance.

3.3 Atomic Oxygen Erosion Yield (E_y)

The atomic oxygen erosion yield (E_y) (cm^3/atom) of the ITO flight samples was determined based on mass loss of the flight samples using dehydrated mass measurements before and after flight. The E_y of the sample is determined through the following equation:

$$E_y = \frac{\Delta M_S}{\left(A_S \rho_S F\right)} \tag{1}$$

where

E_y = erosion yield of flight sample (cm^3/atom)
ΔM_S = mass loss of the flight sample (g)
A_S = surface area of the flight sample exposed to AO (cm^2)
ρ_S = density of flight sample (g/cm^3)
F = low Earth orbit AO fluence ($atoms/cm^2$)

The dehydrated mass was determined using vacuum desiccators following the technique described in Reference 7 using a Sartorius ME 5 Microbalance (1×10^{-6} g sensitivity). The exposed surface area of the flight samples was determined post-flight by taking measurements of the MSC deck sample openings for each flight sample using electronic digital calipers.

4.0 MISSE-9 Mission Exposure

Samples were flown in three different flight orientations during the MISSE-9 mission: ram, with the exposed sample surface windward, facing directly into the flight direction; wake, with samples facing leeward, opposite of the flight direction; and zenith, with samples parallel to the flight direction, facing away from the Earth, out into space. To enable these different orientations, samples were placed on different MISSE Sample Carriers (MSCs); this also means samples in different orientations can be deployed and retrieved at different times. The MSCs open and close like suitcases; the half that is fixed is called the "mount side" (MS), while the half that swings open is called the "swing side" (SS). All ITO samples were located on the mount side of their respective carriers. Relevant mission launch dates, MISSE-FF installation and retrieval, and mission return dates for the MSCs are summarized in Table 2 [3].

Table 2. PCE-1 MISSE-9 Mission Launch and Return [3]

Flight Direction	MISSE Sample Carrier (MSC)	Launch Mission	Installed on MISSE-FF	Retrieved from MISSE-FF	Return Mission
Ram	R2 (MSC 3) MS	SpaceX-14 April 2, 2018	April 18, 2018	Nov. 11, 2019	SpaceX-19 Jan. 7, 2020
Wake	W3 (MSC 8) MS		April 18, 2018	April 26, 2019	SpaceX-17 June 3, 2019
Zenith	Z3 (MSC 5) MS		April 19, 2018		

Figure 3 shows the SpaceX's Dragon capsule loaded with the MISSE-9 ITO samples being captured by ISS's robot arm and later the robot arm being used to attach a blue MISSE-9 MSCs to the MISSE-FF on the outside of ISS. Figure 4 provides images of the MISSE-FF on the ISS Express Logistics Carrier-2 Site 3 (ELC-2 Site 3).

Table 3 provides the PCE-1 MISSE-9 space environmental exposure details for each MSC and includes the flight direction, space vacuum duration, time on the MISSE-FF, direct space exposure duration, atomic oxygen fluence, and the computed mission solar exposure in equivalent sun hours (ESH) [8,9]. Additional flight and MISSE related details can be found in References 3 and 8. Note from Table 3 that the direct space exposure duration for the ram samples was greater than the wake or zenith MSCs. This is due to the carriers being retrieved at different times. The time samples are fully exposed to LEO is not the same as the time the samples have been out on ISS attached to the MISSE-FF because after mounting the MISSE-FF the carrier cases are usually not opened immediately, and carriers also need to be closed occasionally during flight for a variety of scientific and logistical reasons.

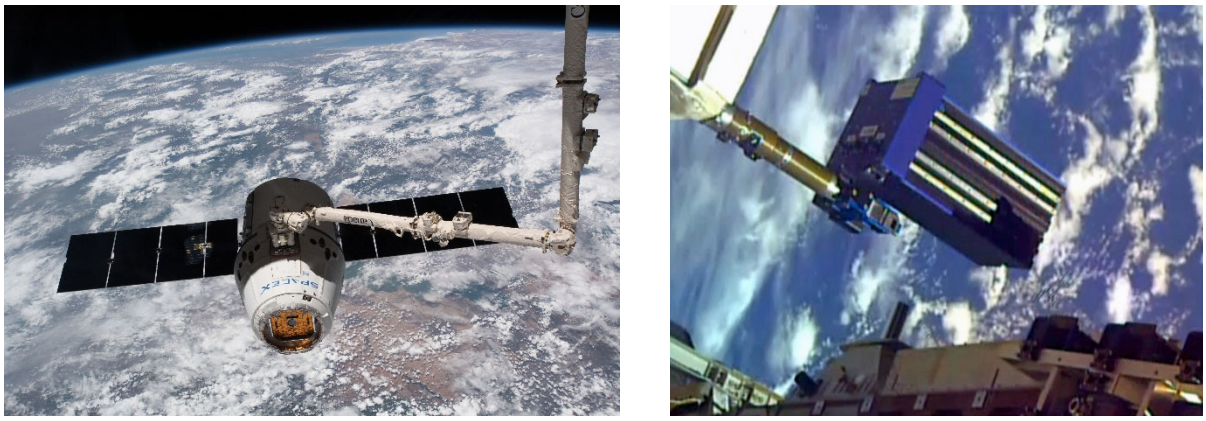

a. b.

Figure 3. Dragon Capsule being captured by the ISS robot arm (a), and the arm being used to attach a MISSE Sample Carrier to ISS (b).

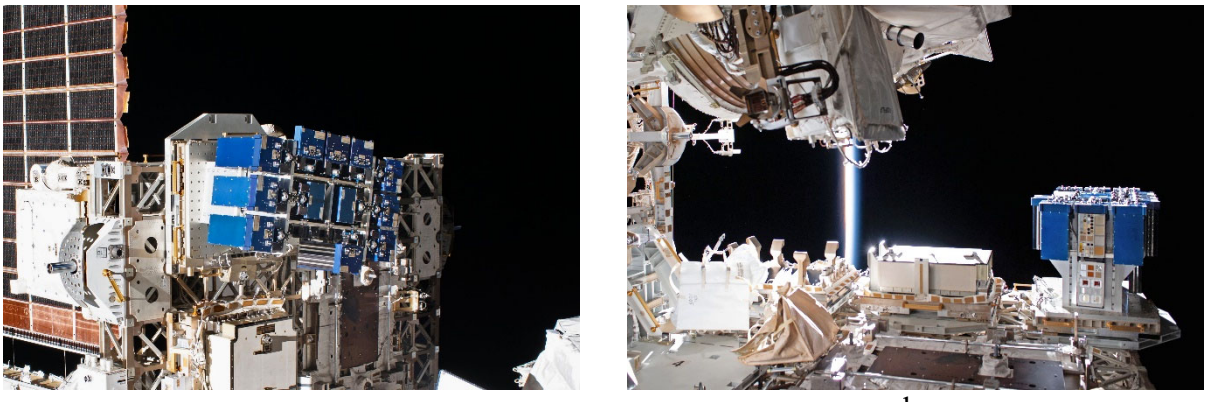

a. b.

Figure 4. Images of the MISSE-FF: (a) View showing the front surface of the ram MSCs (left), and (b) View of the wake MSCs with the center carrier open.

Table 3. PCE-1 MISSE-9 Space Environment Exposure [8,9]

MISSE-FF Experiment	Flight Direction	Space Vacuum Duration (Years)	Time on MISSE-FF (Years)	Direct Space Exposure Duration (Years)	Atomic Oxygen Fluence (atoms/cm^2)	Mission Equivalent Sun Hours (ESH)
MISSE-9 PCE-1	Ram	1.59	1.57	0.77	3.44E+20	952.3
	Wake	1.07	1.02	0.54	4.46E+16	634.6
	Zenith	1.07	1.02	0.54	3.19E+18	555.7

5.0 Results

5.1 Post-Flight Images

Examples of post-flight optical images of the MISSE-9 ITO samples are provided in Figure 5. Because these samples are highly reflective, they can appear bright or dark depending on the lighting conditions. Figure 5 shows two flight samples compared to their un-exposed backups (control samples) using similar lighting. When comparing the flight and control samples of M9W-S1, the samples may appear dark or light as shown in Figure 5b and 5c.

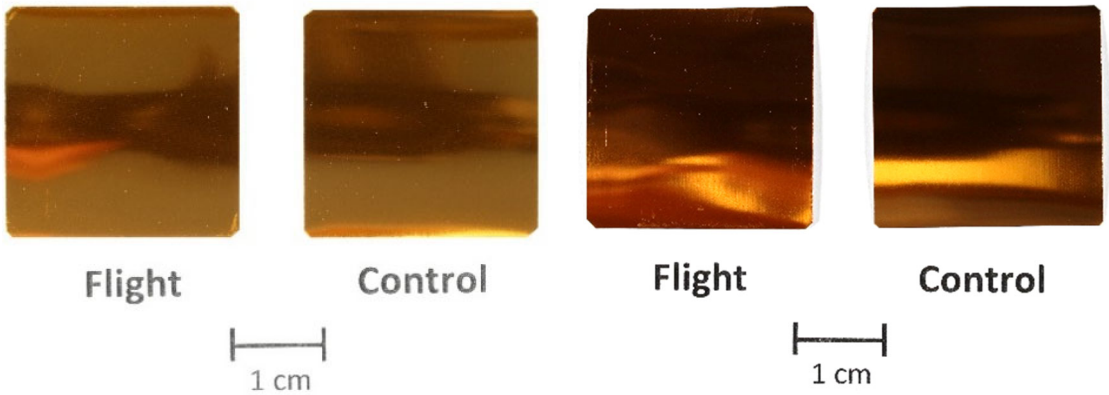

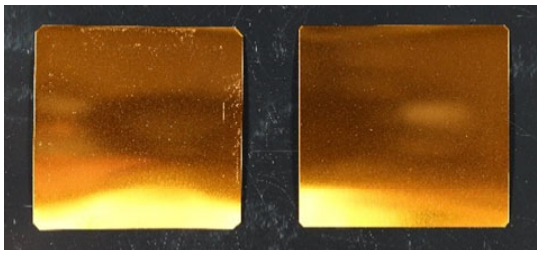

c.

Figure 5. Examples of post-flight images showing the variation in sample appearance with lighting conditions: (a) M9R-S5 ram flight and control, (b) M9W-S1 flight and control under lighting condition 1, and (c) M9W-S1 flight (left) and control (right) under lighting condition 2.

In addition to taking post-flight visible light image photographs of the flight and control samples, images were also taken with a 365 nm wavelength UV light source. Figures 6 to 8 provides post-flight images of all the flight and control samples. Under normal light, the visual differences between the exposed flight samples and unexposed control samples were miniscule as can be seen in Figures 6 to 8. The main visual affect is some perimeter damage from the sample holder on some of the samples, such as shown in Figure 7c and 7e. Structurally, all sheet materials appear to be durable to LEO. The UV images are also provided in Figures 6 to 8. The chemical and structural changes that can occur due to space exposure can influence a material's response to UV light. The post-flight UV light images shows that space exposure did not affect the ITO coated Kapton/Al sheets' response to UV light (see Figure 6b and Figure 7b). However, the UV did cause a small amount of fluorescence for the ITO coated FEP/Ag/Inconel material; the amount of fluorescence appears to increase with AO exposure as shown comparing Figures 6d, 7d, 7f, and 8b.

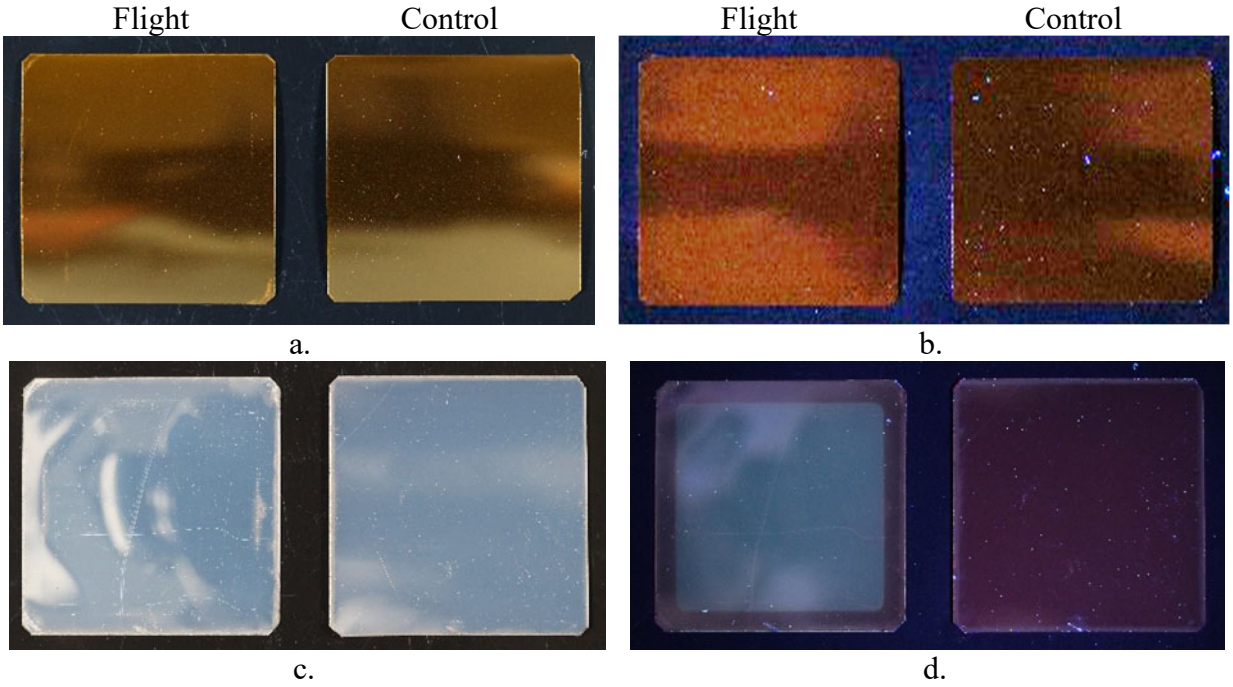

Figure 6. Post-flight normal light and UV luminescence images of the MISSE-9 ram ITO samples: (a) M9R-S5 flight (left) and control (right) under normal visible light, (b) M9R-S5 flight (left) and control (right) under UV light, (c) M9R-S6 flight (left) and control (right) under normal visible light, and (d) M9R-S6 flight (left) and control (right) under UV light.

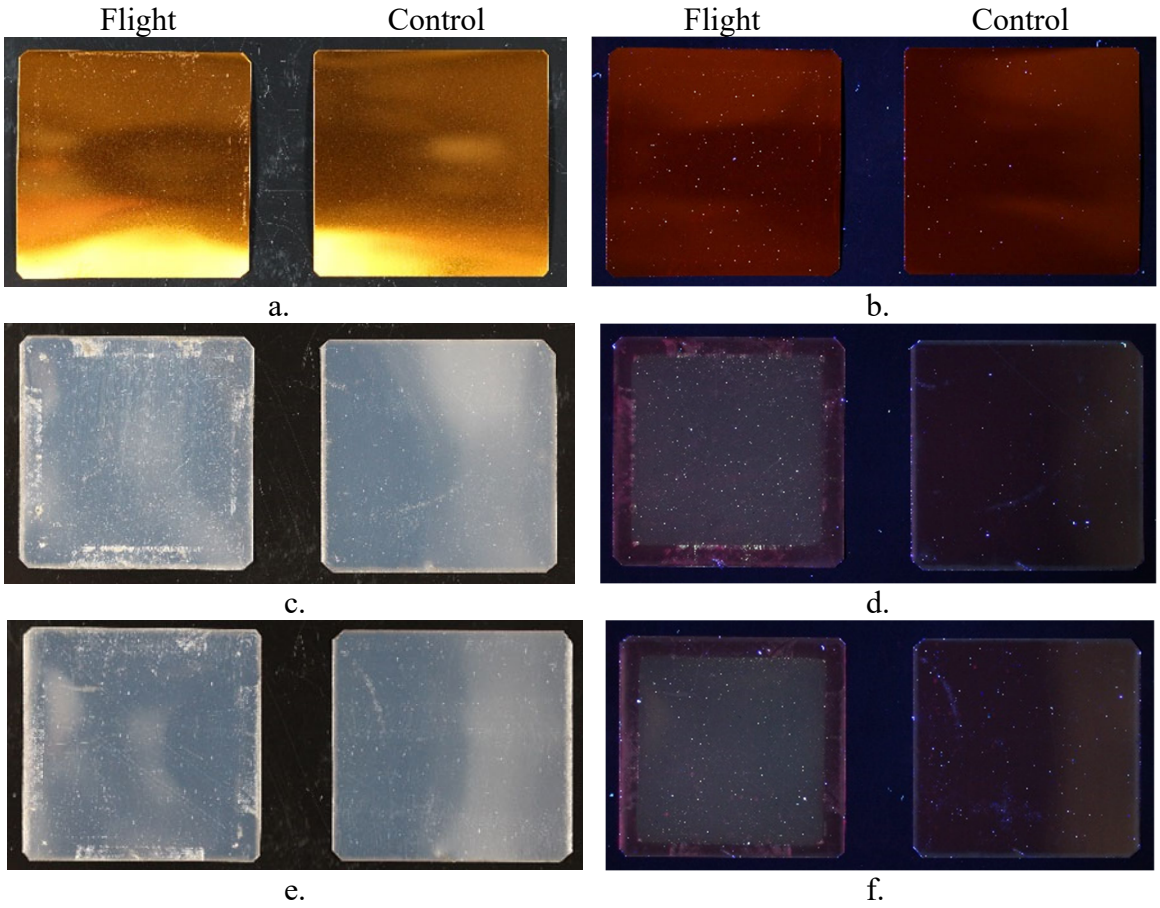

Figure 7. Post-flight normal light and UV luminescence images of the MISSE-9 wake ITO samples: (a) M9W-S1 flight (left) and control (right) under normal visible light, (b) M9W-S1 flight (left) and control (right) under UV light, (c) M9W-S2 flight (left) and control (right) under normal visible light, (d) M9W-S2 flight (left) and control (right) under UV light, (e) M9W-S3 flight (left) and control (right) under normal visible light, and (f) M9W-S3 flight (left) and control (right) under UV light.

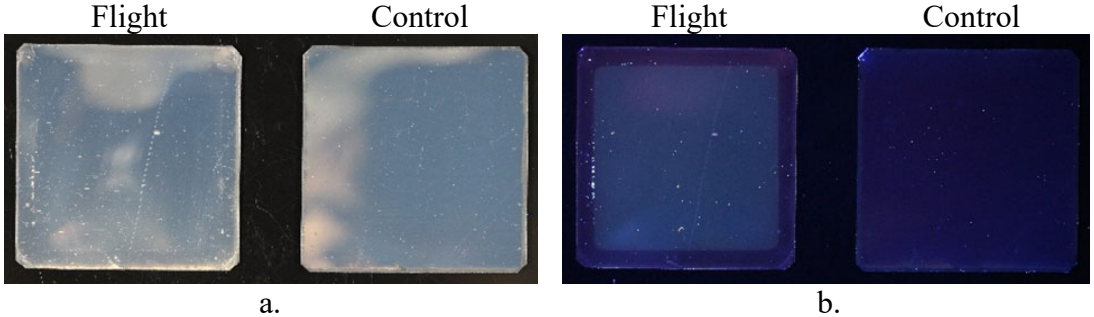

Figure 8. Post-flight normal light and UV luminescence images of the MISSE-9 zenith ITO sample: (a) M9Z-S5 flight (left) and control (right) under normal visible light, and (b) M9Z-S5 flight (left) and control (right) under UV light.

5.2 Sheet Resistance of ITO Sheet Materials Exposed to LEO

Table 4 provides the sheet resistance measurements for the ITO flight and backup samples. The last column in Table 4 lists the average for each backup material. For example, since M9R-S5 Backup and M9W-S1 Backup were cut from the same sheet, these data were averaged and listed in the last column for comparison to their corresponding exposed samples (M9R-S5 Flight and M9W-S1 Flight). We can see that sheet resistance for the ram flight sample M9R-S5 Flight doubled, while the wake sample, M9W-S1 Flight, was not affected by its time in LEO. This is an indication that AO is responsible for the degradation of conductivity of the M9R-S5 flight sample since it flew in the ram orientation and received more AO. The scatter among the resistance measurements for the ITO/FEP/Ag/Inconel sheets was immense, however the levels of resistance increase for ITO/FEP/Ag/Inconel sheets were consistently higher than for ITO/Kapton HN/Al. The absolute resistance values for the ITO/Kapton HN/Al sheets post exposure were also lower than those for ITO/FEP/Ag/Inconel.

5.3 Optical Properties

The air mass zero (AM0) integrated total hemispherical reflectance and solar absorptance results are provided in Table 5. The solar absorptance spectra for the flight and control samples are provided in Figures 9 to 14. As can be seen in Table 5, there were very small, or no, change in the integrated AM0 solar absorptance values of the flight samples as compared to the controls. The largest increase in solar absorptance was for the M9Z-S5 F zenith sample, which increased in solar absorptance by only 0.002, which is within error of the Cary data. As can be seen in Figures 9 to 14, the absorptance spectra comparisons, there are very small decreases in the IR regions and increases in the UV regions for the flight samples as compared to the controls.

5.4 Atomic Oxygen Erosion Yield (E_y)

The atomic oxygen erosion yield (E_y) values for the MISSE-9 ITO samples are provided in Table 6 along with the samples mass loss (dehydrated), exposed surface area, density, and mission AO fluence. All samples had little mass loss. The Kapton H films had slightly greater mass loss than the FEP films. The mass loss for the M9W-S2 F, M9W-S3 F and M9Z-S5 F are within the Sartorius ME5-2 Microbalance error (±0.005 mg). The M9R-S6 F sample mass loss is just slightly above the error range. Thus, none of the MISSE-9 ITO coated Silver-Teflon samples lost any significant mass.

Table 4. MISSE-9 PCE-1 ITO Samples Sheet Resistance

MISSE-9 ID	Material Abbreviation	Resistance, Ohm/square									Average	Overall Average for Unexposed Material
Ram												
M9R-S5 **Flight**	ITO/Kapton HN /Al	13,000	13000	10,000	9,100	9,000					10,820	
M9R-S5 Backup	ITO/Kapton HN /Al	7,000	5700	5,200	5,300	4,100					5,460	5,230
M9R-S6 **Flight**	ITO/FEP/Ag/ Inconel	70,000	73000	70,000							71,000	
M9R-S6 Backup	ITO/FEP/Ag/ Inconel	10,000	23000	15,100	12,700	8,100	6,500	5,800	4,900	4,700	10,089	7,296
Wake												
M9W-S1 **Flight**	ITO/Kapton HN /Al	5,000									5000	
M9W-S1 Backup	ITO/Kapton HN /Al	5,000									5000	5,230
M9W-S2 **Flight**	ITO/FEP/Ag/ Inconel	8,800	22700	22,700	21,100	4,100	2,100	15,500	13,800	13,500	15,880	
M9W-S2 Backup	ITO/FEP/Ag/ Inconel	3,520	4500	3,300	3,170	2,940	2,800				3,486	7,296
M9W-S3 **Flight**	ITO/FEP/Ag/ Inconel	9,700	379000	381,000	27,900	28,000					165,120	
M9W-S3 Backup	ITO/FEP/Ag/ Inconel	4,700	5500	4,200	4,120	4,070					4,518	7,296
Zenith												
M9Z-S5 **Flight**	ITO/FEP/Ag/ Inconel	5,000	7100	6,700	8,400	7,800					7,000	
M9Z-S5 Backup	ITO/FEP/Ag/ Inconel	3,800	10300	17,100	12,500	11,760	2,780	2,580	2,480		11,092	7,296

Table 5. MISSE-9 PCE-1 ITO Samples Optical Properties

Material	MISSE ID	Flight Orientation	AM0 Total Reflectance			AM0 Solar Absorptance		
			Control	LEO Exposed	Change	Control	LEO Exposed	Change
ITO/Kapton HN/Al	M9R-S5 B		0.577			0.423		
	M9R-S5 F	Ram		0.580	0.003		0.420	-0.003
	M9W-S1 F	Wake		0.578	0.001		0.422	-0.001
ITO/FEP/Ag/Inconel	M9W-S2 B		0.902			0.098		
	M9R-S6 F	Ram		0.907	0.005		0.093	-0.005
	M9W-S2 F	Wake		0.901	-0.001		0.099	0.001
	M9W-S3 F	Wake		0.904	0.002		0.096	-0.002
	M9Z-S5 F	Zenith		0.900	-0.002		0.100	0.002

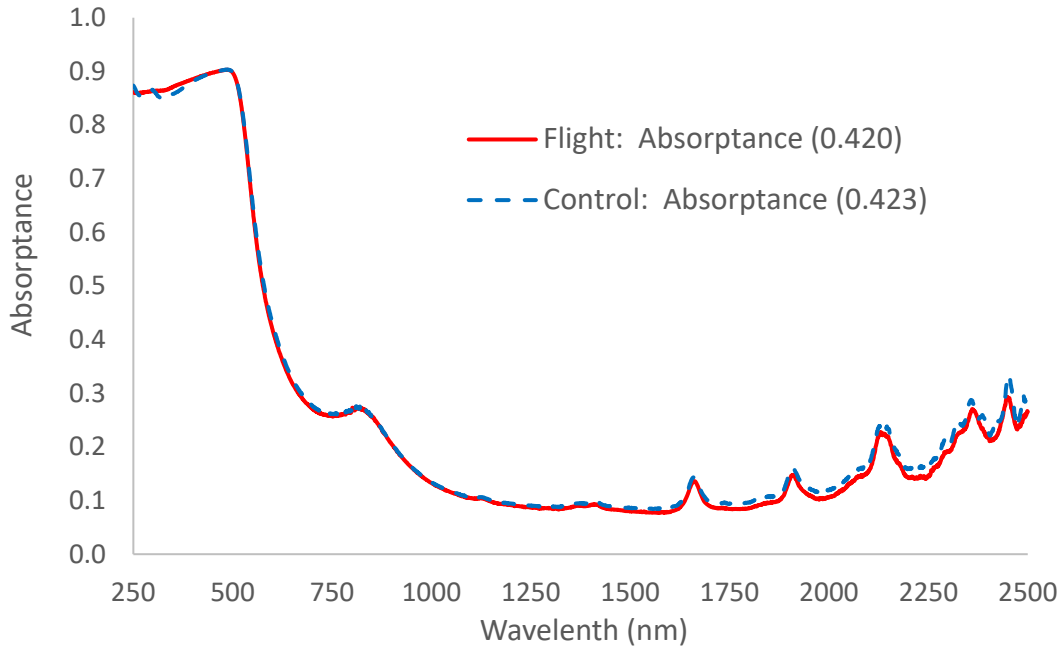

Figure 9. Absorptance spectra for M9R-S5 (ITO/Kapton HN/Al) ram flight and control samples.

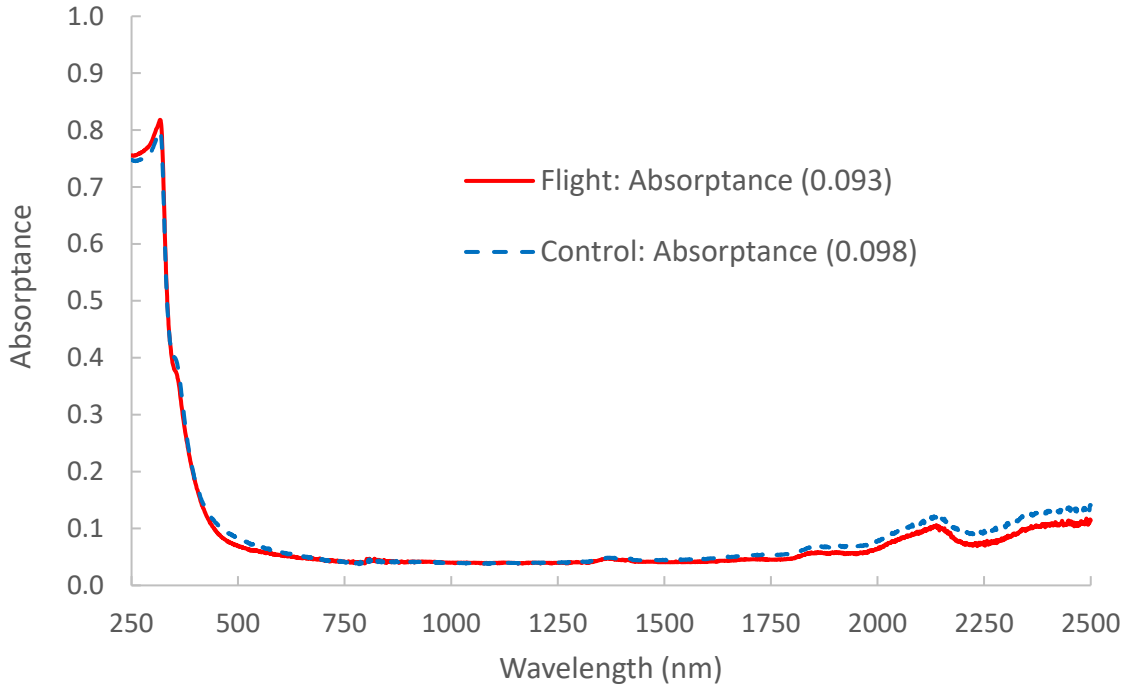

Figure 10. Absorptance spectra for M9R-S6 (ITO/FEP/Ag/Inconel) ram flight and control samples.

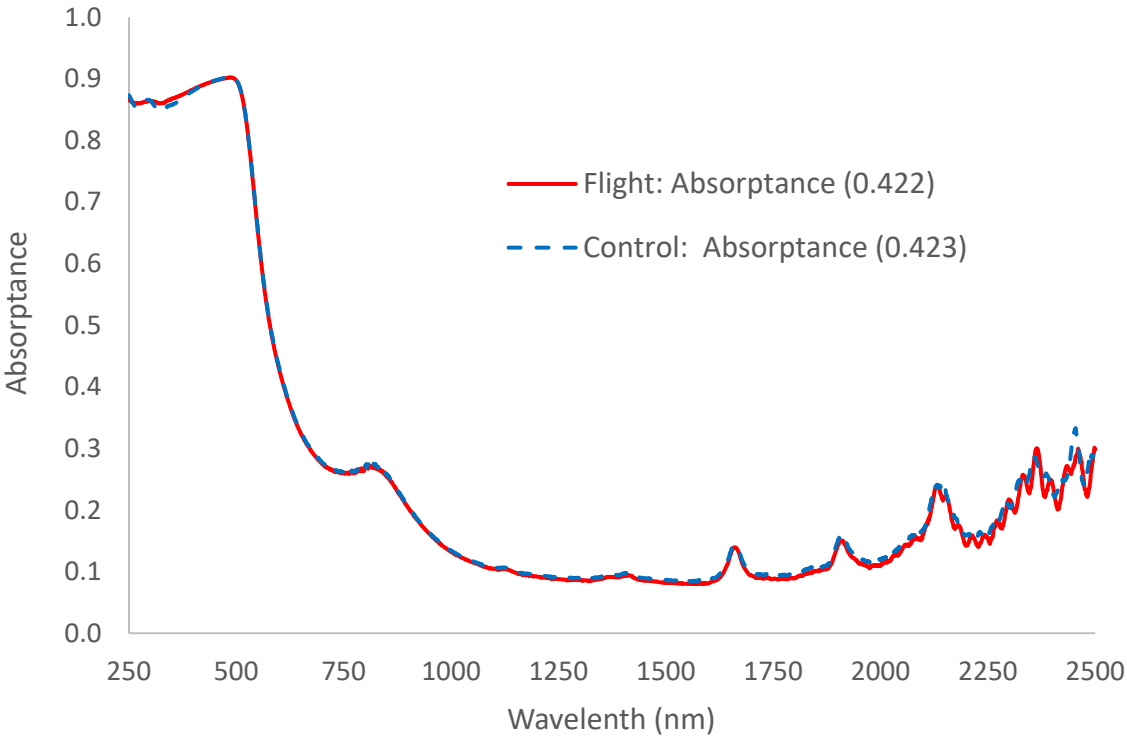

Figure 11. Absorptance spectra for M9W-S1 (ITO/Kapton HN/Al) wake flight and control samples.

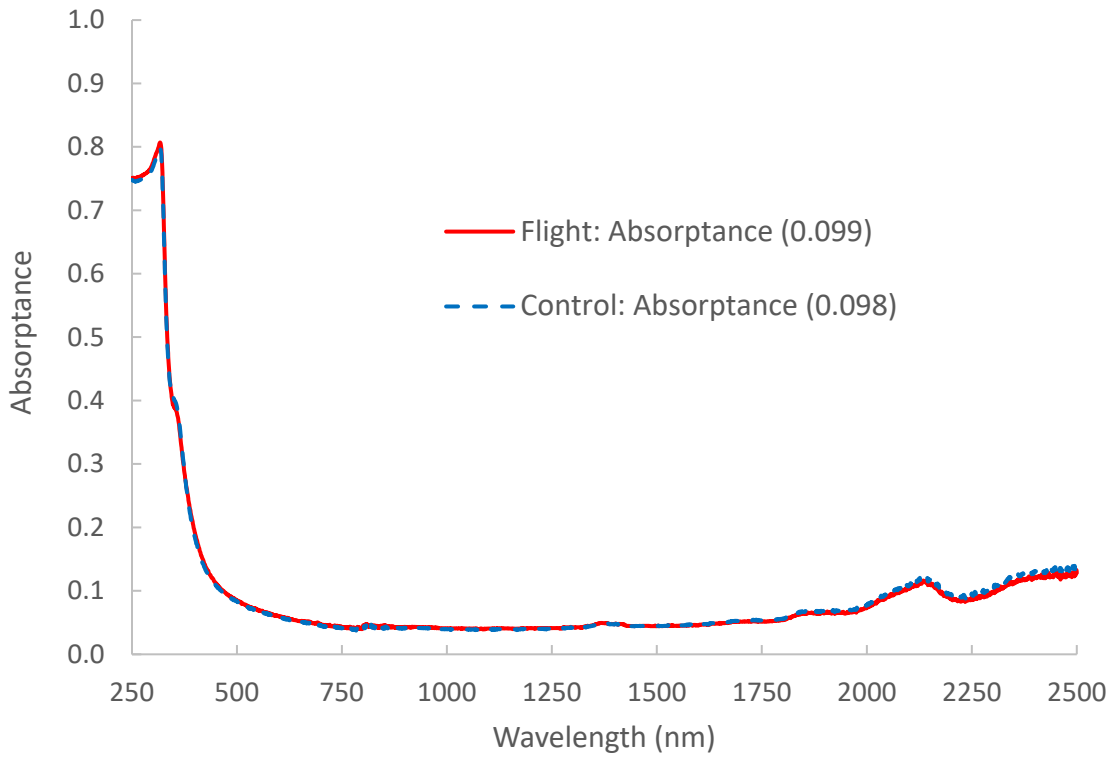

Figure 12. Absorptance spectra for M9W-S2 (ITO/Kapton HN/Al) wake flight and control samples.

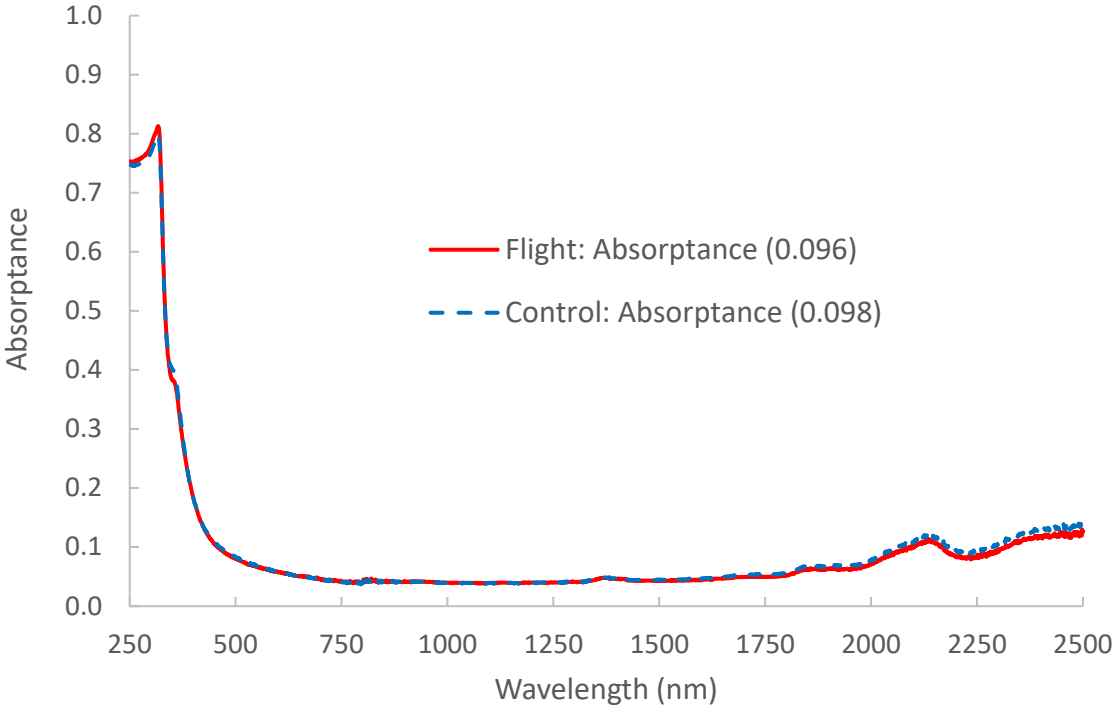

Figure 13. Absorptance spectra for M9W-S3 (ITO/FEP/Ag/Inconel) wake flight and control samples.

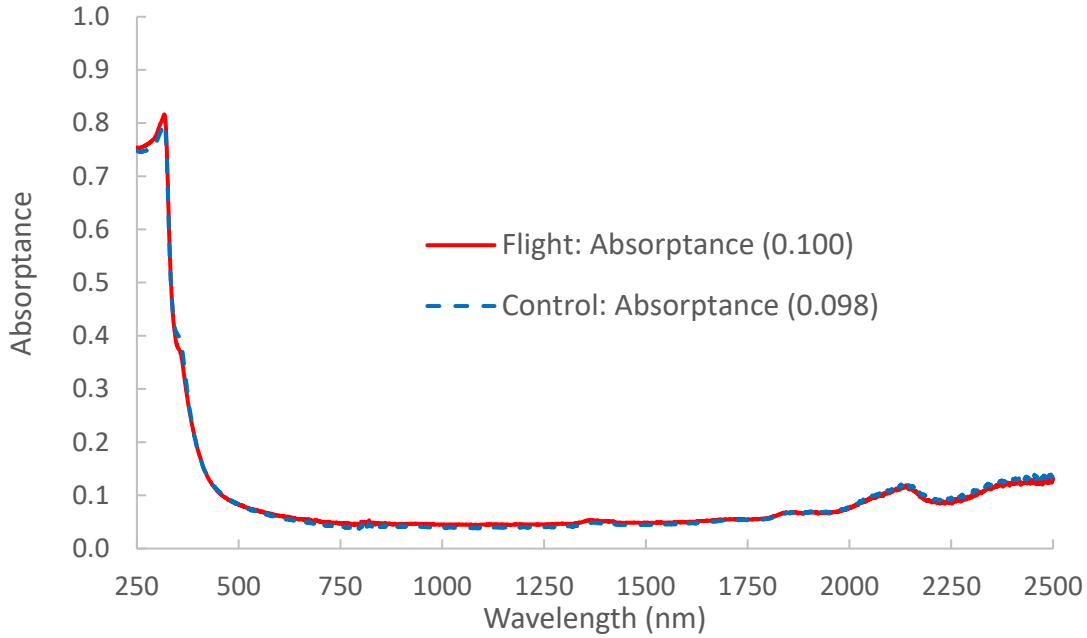

Figure 14. Absorptance spectra for M9Z-S5 (ITO/FEP/Ag/Inconel) zenith flight and control samples.

Table 6. MISSE-9 AO Mass Loss and Erosion Yield

MISSE-9 ID	Abbreviation	Thickness (mils)	Mass Loss (g)	Surface Area (cm^2)	ITO Density [10] (g/cm^3)	MISSE-9 AO Fluence [8] ($atoms/cm^2$)	MISSE-9 E_y ($cm^3/atom$)
MISSE-9 PCE-1 Ram ITO Samples							
M9R-S5 F	ITO/Kapton HN/Al	2	0.000069	4.414	6.8	3.44E+20	6.72E-27
M9R-S6 F	ITO/FEP/Ag/Inconel	5	0.000009	4.420	6.8	3.44E+20	9.04E-28
MISSE-9 PCE-1 Wake ITO Samples							
M9W-S1 F	ITO/Kapton HN/Al	2	0.000043	4.406	6.8	4.46E+16	3.19E-23
M9W-S2 F	ITO/FEP/Ag/Inconel	5	0.000003	4.387	6.8	4.46E+16	2.00E-24
M9W-S3 F	ITO/FEP/Ag/Inconel	5	0.000002	4.416	6.8	4.46E+16	1.74E-24
MISSE-9 PCE-1 Zenith ITO Samples							
M9Z-S5 F	ITO/FEP/Ag/Inconel	5	0.000001	4.501	6.8	3.19E+18	6.83E-27

6.0 Conclusions

Six ITO coated thin film samples were flown as part of the PCE-1 flight experiment during the MISSE-9 mission. Samples were flown in ram, wake, and zenith flight orientations, and received 0.77, 0.54 and 0.54 years of space exposure, respectively. All ITO coated sheets performed well and were not noticeably damaged by their time in LEO implying they are suitable for use as thermal control sheet materials. The AO erosion yields were very low, and the integrated AM0 solar absorptance for the samples changed very little, if at all. Although the sheet resistance of the ITO coated Kapton HN/Al doubled after ram oriented space exposure, its final resistance of 10,820 Ohm/square is believed to be low enough to provide dissipation of electrostatic charges. Sheet resistance measurements for the ITO coated FEP/Ag/Inconel sheets were much less consistent, suffering from high levels of scatter, with a few resistance measurements being very high (>370,000 Ohms/square). It is recommended that the sheet resistance of all samples be measured again using calibrated equipment.

References

1. Reddy, I. N., Reddy, V. R., Sridhara, N., Rajendra, A., Rao, V. S., Dey, A. and Sharma, A. K., "Development and environmental stability of ITO thin film for spacecraft application," Materials Research Innovations, 17(1): 22–26, February 2013.
2. Goldstein, R. D., Brown, E. M. and Maldoon, L. C., "Usage of ITO to Prevent Spacecraft Charging," IEEE Transactions on Nuclear Science, vol. NS-29, no. 6, December 1982.
3. de Groh, K. K. and Banks, B. A., "MISSE-Flight Facility Polymers and Composites Experiment 1-4 (PCE 1-4)," NASA/TM-20205008863, February 2021.
4. "*Spacecraft Polymers Atomic Oxygen Durability Handbook*," de Groh, K. K., Banks, B. A. and McCarthy, C. E., NASA–HDBK–6024, 2022.
5. "U.S. Standard Atmosphere, 1976," National Aeronautics and Space Administration, NASA TM–X–74335, 1976.
6. 2000 ASTM Standard Extraterrestrial Spectrum Reference E-490-00, http://rredc.nrel.gov/solar/spectra/AM0.
7. de Groh, K. K. and Banks, B. A., "Atomic Oxygen Erosion Data from the MISSE 2-8 Missions," NASA/TM-2019-219982, May 2019.
8. de Groh, K. K. and Banks, B. A., "Space Environmental Exposure of the MISSE 9-15 Polymers and Composites Experiment 1-4 (PCE 1-4)," NASA/TM-20240000755, February 2024.
9. Aegis Aerospace's "MISSE MSC UV Equivalent Sun Hours Calculation," Report (A. Goode, MEMO-MISSE-0004 Rev C03, August 17, 2022).
10. Journal Vac. Sci. Tech A 19:5(2043-7); 2001.